2. Planar bioimpedance probes

An outstanding novelty of this thesis work is the use of a needle shaped silicon probe for bioimpedance measurements. This chapter justifies its design, particularly those issues related to the planar configuration of the electrodes in comparison to previous designs, and also describes its main features. It is shown that a non-constant inter-electrode separation distance configuration not only enhances sensitivity but it also improves spatial resolution.

Special attention is given to the electrode-tissue interface impedance. The commonly used 'platinization' process for interface impedance reduction has been adjusted for the electrode sizes and the application. That has implied higher current densities for the electrochemical deposition and the use of ultrasonic agitation. The electrode-tissue interface impedance was measured *in vivo* and it was observed that its heterogeneity is much larger than that obtained in the case of saline solutions.

Probes based on flexible materials are also briefly introduced and characterized.

The annexes B and D are related to the contents of this chapter.

2.1. Previous bioimpedance probes

Probably, the most critical issue concerning bioimpedance measurement is the electrical connection between the instrumentation and the sample under study.

Excluding some measuring solutions based on contactless strategies such as magnetic coupling [1;2] or open-ended coaxial probes [3;4], most bioimpedance measurements are performed through electrodes. As it is explained in the next chapter, in the case that bioimpedance measurements at low frequencies are required, the impedance features of the electrode interface almost force the adoption of the four-electrode method.

There are some four-electrode measurement chambers intended for excised tissues or cells that are not appropriate at all for *in vivo* or whole tissue studies. These measurement cells, on the contrary, are considered specially suitable for accurate measurements because they show excellent features concerning the uniformity of the electrical fields. For instance, Figure 2.1 shows a measurement cell intended for measuring the dielectric parameters of human erythrocytes.

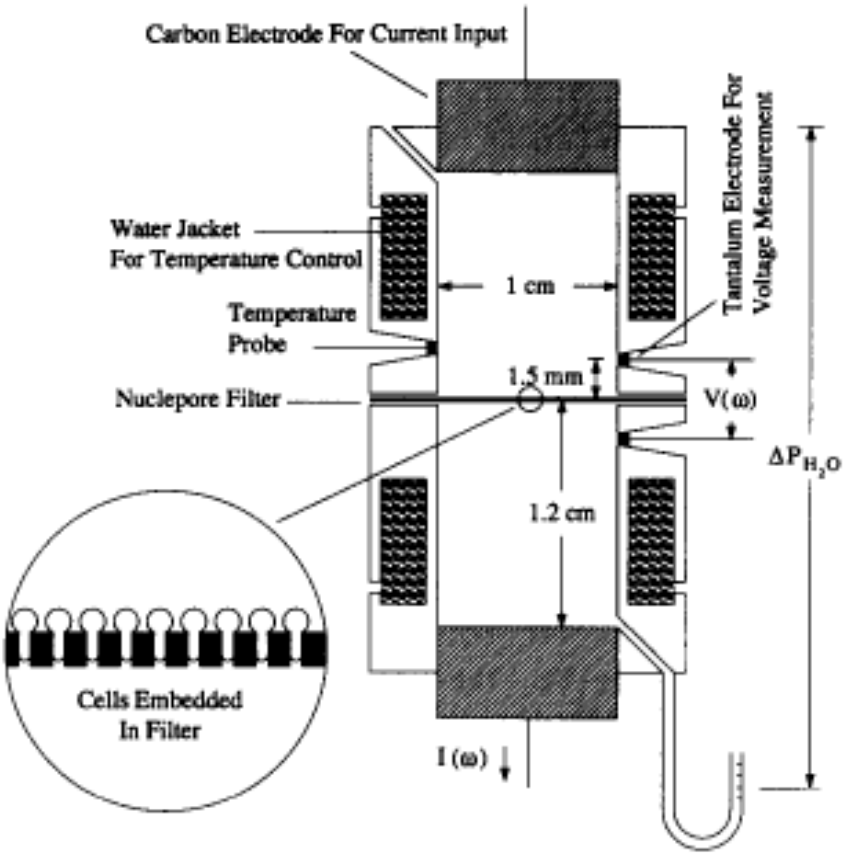

Figure 2.1. Electrical impedance measurement chamber for human erythrocytes (source: [5]).

When performing bioimpedance measurements of the whole body, of the thorax or of the extremities, the most common electrode configurations are based on metallic electrodes (noble metals or stainless steel) or electrolytic gel electrodes (standard ECG electrodes). These electrodes, in the shape of plates or bands, are attached to the surface of the sample under study in such a way that maximizes the measured impedance changes due to the physiological event that needs to be monitored [6]. Unfortunately, this sort of configuration is too much prone to measurement artifacts since any movement of the sample causes a change of the cell geometry and this, in turn, modifies the measured value. This fact makes it difficult to use such configurations for *in vivo* organ studies since in most cases it is not possible to guarantee the static condition. Moreover, other two facts make things even more difficult: 1) in an *in vivo* tissue it is not always possible to place the electrodes on the sample surface position required to maximize the impedance signal and 2) the presence of plasma or blood around the tissue under study can create a short-circuit and impede the measurements. However, some successful solutions based on flat electrodes fixed to a rigid structure that somehow is attached to the sample have been proposed [7;8]. The solution given by Steendijk et al.[7] (see Figure 2.2) solves the attachment issue by using a suction cup that maintains the electrodes in close contact with the tissue surface and also avoids, in part, the presence of plasma or blood. Nevertheless, the resulting device cannot considered to be minimally invasive since the suction damages, or at least alters, the living tissue. Furthermore, as it will be shown later, these sort of configurations based on planar electrodes imply an important limitation: the effective measurement volume is mostly constrained at the tissue surface and, therefore, electrical properties of the inner tissue cannot be measured.

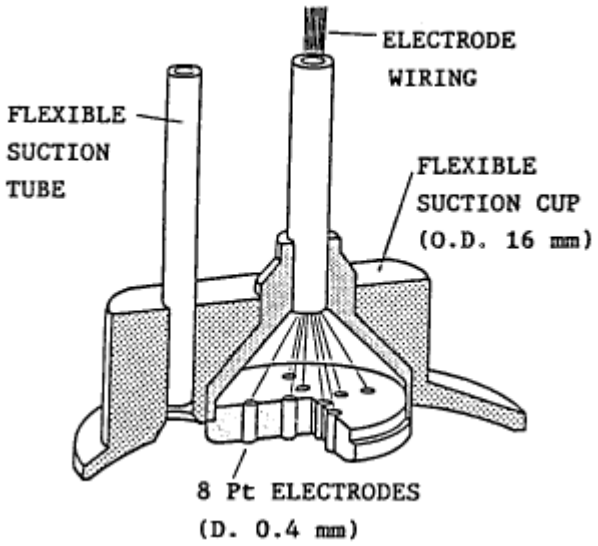

Figure 2.2. Bioimpedance probe consisting of two electrode arrays of four electrodes in a flexible suction cup.

Because of the above mentioned problems, the impedance probe used in most *in vivo* studies consists in an array of four equidistant needle shaped electrodes (see Figure

2.3). The outer electrodes are employed to inject the AC current into the tissue and the resulting potential is differentially measured across the inner electrodes [9].

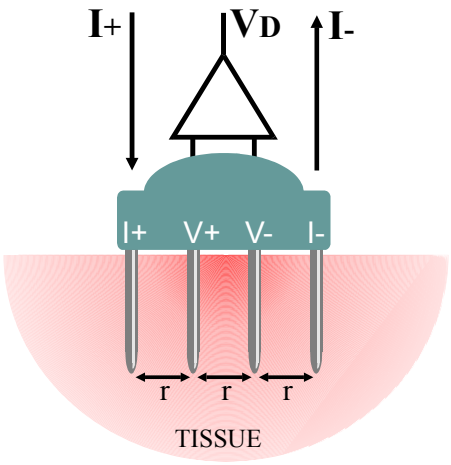

Figure 2.3. Classical four electrode-plunge probe.

Although the four-electrode plunge probe has been used by many researchers [10-17] and its feasibility to perform bioimpedance measurements has been sufficiently demonstrated, there are some practical issues that limit its clinical applicability:

- fabrication process results in large tolerances because of the critical positioning and alignment of the electrodes.
- damage caused to the tissue is considerable since each probe causes four punctures to the tissue.
- presence of blood or plasma surrounding the tissue can shunt the electrodes and disturb the measurements [7].
- there is a strong dependence of apparent resistance on insertion depth [18].

Therefore, the clinical use of bioimpedance measurements to monitor the condition of loving tissues is not still a reality.

2.2. Silicon probe for electrical bioimpedance measurements

As it was pointed out in the introduction, the idea of the MicroCard project was to include multiple sensors on a silicon probe together with the conditioning and transmitting electronics. However, in order to proceed in a efficient way, at the beginning the different elements were designed and implemented separately with the idea of later integration. In the case of bioimpedance, a needle shaped probe with four aligned platinum electrodes on its surface was designed and implemented (see Figure 2.4).

Silicon needle shaped probes with planar electrodes on their surfaces had been developed previously for neuronal activity recording [19-22], but, as far as we know, they had never been used for four-electrode impedance measurements.

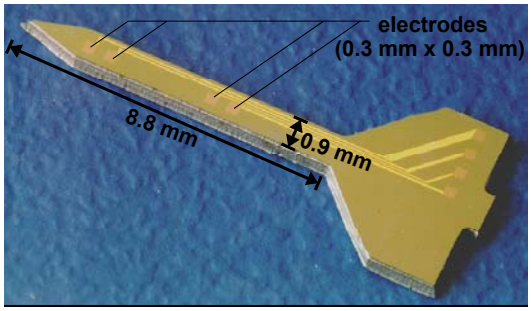

Figure 2.4. First silicon bioimpedance probe prototype

The design of this first probe was carried out by Prof. José Millán, Dr. Mark Warren and Dr. Philippe Godignon and was based on knowledge of the classical plunge probes and some intuitive ideas. The plunge probe successfully used by the Dr. Cinca team consisted of four platinum needle electrodes (5 mm long, 0.4 mm diameter) mounted in a linear array on an insulating substrate separated by an inter-electrode distance of 2.5 mm. As it can be observed, there were some clear differences between both designs. The following table compares some features of both probes.

Table 2.1. Comparison between the plunge probe used by Dr. Cinca team and the silicon probe.

	plunge probe	**silicon probe**
array length	7.5 mm	4 mm
electrode material	Pt	Pt
electrode area	~6.3 mm^2	0.09 mm^2
electrode separation	constant (2.5 mm)	non constant

The main reasons that justify the silicon probe design are summarized below:

- The silicon probe must be inserted perpendicular to the tissue and, in the case of the heart, that implies a limitation to the probe length because of the myocardium

thickness (<1 cm). Thus, taken into account that and the fact that the electrodes needed to be at some distance from the tissue surface, it was decided to reduce the array length from 7.5 mm to 4 mm.

- The separation distance between the inner electrodes (voltage electrodes) was increased in order to increase the voltage drop and improve the signal to noise ratio. This intuitive strategy was not analyzed at those moments but probed to be experimentally useful and, as it is shown later, a theoretical analysis demonstrated its advantages [23].

- The fact that the electrodes are square shaped implies that electric fields are larger around the vertexes (non-uniform fields) and that non-linear effects of the tissue or the electrode-electrolyte interface impedance[1] will be manifested more easily. These undesired effects could be minimized by employing circular electrodes but, in that case, the available electrode area would be reduced for a given needle shaft width.

- The track areas were designed in order to minimize the resistance from the electrodes to the bonding pads. Furthermore, the tracks for the two inner electrodes (voltage measuring electrodes) were designed in such a way that they had equal resistance values [2].

- The bonding pads (300 μm × 300 μm) were larger than usual (100 μm × 100 μm) in order to be able to use non-standard bonding techniques such as silver filled epoxies or conductive adhesives.

- The technological process determined the substrate material (Si) and the isolating materials (SiO_2 and Si_3N_4). The chosen electrode material was platinum because of its biocompatibility and its low electrode-electrolyte interface impedance compared to other materials such as stainless steel or silver.

This probe was experimentally tested by Dr. Cinca team with positive results [24]. The bioimpedance measurements at 1 kHz were comparable to those obtained with their own plunge probe (Figure 2.5). However, occasionally they obtained distorted responses that were presumably caused by large electrode interface impedances. Moreover, the probe was not suitable for the *in vivo* detection of the onset of myocardial ischemia because it incidentally caused significant bleeding.

[1] See next chapter.

[2] The importance of that is seen in next chapter.

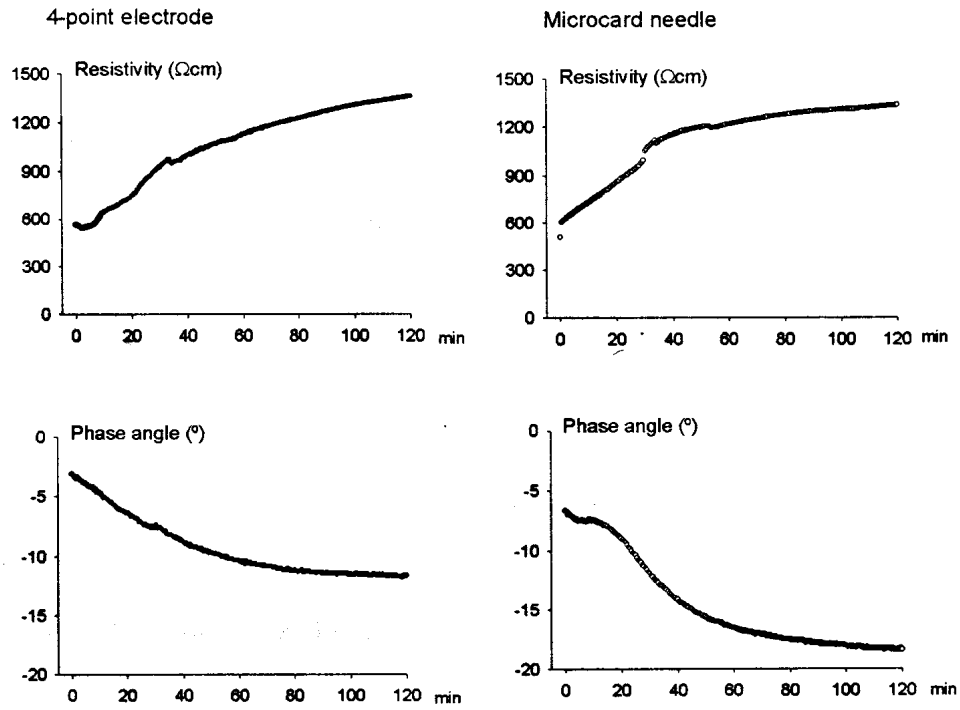

Figure 2.5. Evolution of the resistivity and phase angle at 1 kHz of explanted porcine myocardium measured with the plunge probe (4-point electrode) and the MicroCard probe, reproduced from [24].

The current MicroCard bioimpedance probe does not differ too much from the first design (Figure 2.4). Apart from the width reduction (from 900 μm to 600 μm), the most significant changes are related to the fabrication of the probe: 1) deep RIE[3] micromachining has been substituted by mechanical micromachining by using a wafer saw and 2) a platinization process is now being used to reduce the electrode-tissue interface impedance (see section 2.2.3). Concerning the design, the tracks from the electrodes to the bonding pads were modified in order to obtain balanced impedances for the voltage measuring electrodes, not only in terms of resistance but also in terms of capacitance.

The original needle shape micromachining by deep RIE implied some important technical problems and a significant delay for MicroCard and MicroTrans projects. Because of that, it was decided to try another method: to use the wafer saw to define the needle shape after all the microelectronic processes have been carried out. Of course, this option limits the number of shapes that can be defined. If it is desired to make an optimum use of the entire wafer area, only trapezoids can be obtained (combination of crossed longitudinal cuts, see Figure 2.6). Fortunately, a trapezoid is just what is needed to implement insertion probes.

[3] RIE stands for Reactive Ion Etching and it is a plasma based dry etching technique that allows high aspect-ratio vertical structures (highly anisotropical etching). Deep RIE (DRIE) uses a two-step cycle (passivation deposition to protect side walls and etching) and allows through-wafer etching [25].

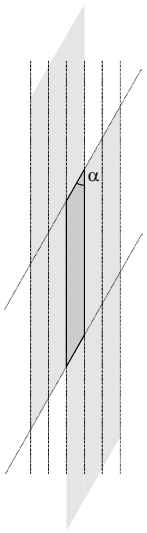

Figure 2.6. Schematic representation of the sawing directions used to obtain the needle shapes.

The advantages of this mechanical machining (MM) process compared to deep RIE are:

- MM is totally compatible with microelectronic processes ⇒ any microelectronic circuitry can be integrated on the needles.
- MM is performed after the wafers have been processed ⇒ contamination problems are avoided.
- MM results in yield improvement ⇒ lower production costs.
- MM costs are much lower ⇒ lower production costs.
- MM is critically faster ⇒ lower production costs.

Moreover, the current impedance probe seldom causes bleeding. Although this improvement could be caused because of the width reduction or the new needle tip shape, it also seems to be related with the smoothness of the side surfaces that is achieved by the wafer saw. Details about the current MicroCard probe fabrication, characterization and its features can be found in Annex D.

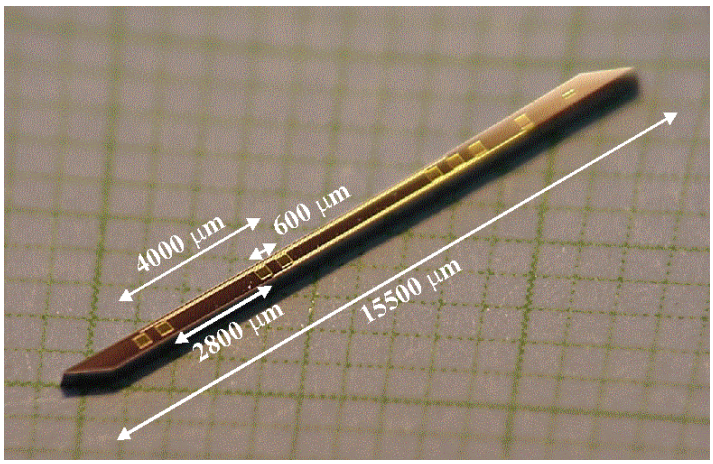

Figure 2.7. Current impedance probe design. The electrode sizes (300 µm × 300 µm) and separation distances are the same than those of Figure 2.4.

2.2.1. Geometrical design of the electrode array

This section analyzes the contribution of the electrode array geometry to the impedance probe performance. Its main objective is to show the consequences of choosing a non-constant inter-electrode separation distance. The analysis is performed considering an array of flat electrodes on a flat surface but most of the conclusions can be applied also for plunge electrodes.

In the case of a constant inter-electrode separation distance (IESD) structure, there are some reasons to minimize the spacing between the electrodes:

1) Signal to noise ratio enhancement. That is, to increase the voltage drop between the inner electrodes for a given sample and a limited current.
The relation between the voltage drop (V), the injected current (I), the sample resistivity (ρ) and the IESD (r) in an isotropic and uniform medium is [7]:

$$V = k\frac{\rho}{r}I \tag{2.1}$$

where k is $(4\pi)^{-1}$ in the case that the medium is infinite and $(2\pi)^{-1}$ in the case that the medium is semi-infinite, that is, the electrode array is applied on the flat surface of a medium which is bounded by another medium with an infinite resistivity such as air.

2) Spatial resolution improvement. Robillard and Poussart [26] determined that impedance measurements are not disturbed by medium transitions at distances beyond 3 × IESD.

3) Probe size reduction and, consequently, tissue damage minimization.

On the other hand, there are also some good reasons for the opposite:

1) Homogeneity. That is, to minimize the scatter of measured values due to the heterogeneity of the living tissues [27]. If electrodes are too much close, the measured impedances will depend on the position of the probe in relation to the cell matrix.
Because of that, an IESD quite larger that the maximum cellular size is advisable (0.2 mm in the case of the skeletal muscle).

2) Blood shunting phenomenon minimization. The presence of a thin layer of blood or serum on the array surface can be the most serious drawback of planar configurations because such a disturbing layer can 'shield' the sample from the probe by short-circuiting the electrodes (Figure 2.8 depicts an schematic representation of such a phenomenon). Steendijk et al. [7] have modeled the influence of these layers and have determined that a layer with a IESD/10 thickness and a resistivity below one tenth of the sample resistivity causes an impedance module error higher than the 20%. If the presence of such a layer cannot be avoided, this error can only be reduced by increasing the IESD/layer thickness ratio.

Figure 2.8. The presence of a low resistivity layer on the electrodes seriously disturbs the bioimpedance measurements.

3) Electrode area enlargement in order to reduce their interface impedance.

4) Parasitic capacitances reduction.

The case of non-constant IESD has not been studied before and *a priori* it is not known what is the effect of reducing the distance between the inner electrodes and the outer electrodes. In the following analysis it is considered that the distance between the inner electrodes is b, the total length array length is $2a+b$ and $a<b$.

Following the same procedure that is described in [13] , an equivalent expression to (2.1) is obtained for the non-constant IESD array[4].

$$V = k\rho \frac{2b}{a(a+b)} I \tag{2.2}$$

This implies that when the distance between the inner and the outer electrodes, a, is reduced whereas the total array length is kept constant, the voltage difference will be increased and the signal to noise ratio will be enhanced. Thus, at it was thought, to reduce the distance between the inner and the outer electrodes will improve the voltage difference.

Spatial resolution and the effect of a disturbing layer on the electrodes are also modified by choosing a non-constant IESD structure. By using the image method as it was previously applied by Robillard and Poussart [26], it is analytically found an expression that provides the apparent resistivity (measured resistivity, ρ') when there exists a transition of two media (ρ_1 and ρ_2) at a distance x from the non-constant IESD array and parallel to the array axis:

$$\rho' = \rho\left(1 + K\frac{G'}{G}\right) \tag{2.3}$$

[4] In the Annex B it is detailed how this and the following expressions presented in this section have been obtained.

$$G = \left(\frac{1}{a} - \frac{1}{a+b} \right) \tag{2.4}$$

$$G' = \left(\frac{1}{\sqrt{4x^2 + a^2}} - \frac{1}{\sqrt{4x^2 + (a+b)^2}} \right) \tag{2.5}$$

$$K = \frac{\rho_2 - \rho_1}{\rho_2 + \rho_1} \tag{2.6}$$

where K is the 'reflection coefficient' and depends on the resistivity of the medium in contact with the array (ρ_1) and on the resistivity of the medium that extends beyond the transition located at x (ρ_2).

These expressions can be applied to determine the spatial resolution. For instance, it is possible to analyze the effect of a non-conductive medium such as air that constrains the medium under study at a distance x from the electrode array (see Figure 2.9). Observe that the distance at which the effect of ρ_2 is manifested is shortened when a is reduced while the array length ($2a+b$) is kept constant. Therefore, bringing the inner electrodes closer to the outer electrodes is beneficial in terms of spatial resolution.

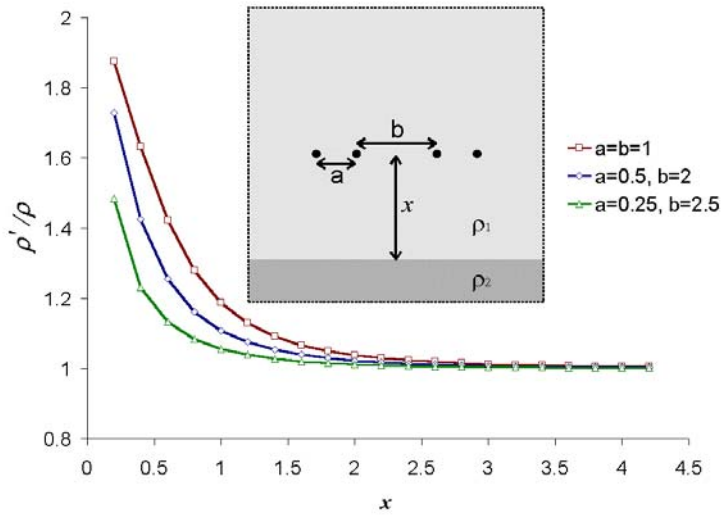

Figure 2.9. Estimated ρ'/ρ (apparent resistivity / infinite extent medium resistivity) of a conductive medium bounded by a non-conductive medium.

The above expressions (Equation 2.3) were deduced under the assumption that the electrodes were point-sized, however, this is not at all the case of the silicon probes since the electrodes sizes are comparable to the separation distances (Figure 2.4, Figure 2.7). For that reason, an experimental set up was implemented to confirm the validity

of the model: a silicon probe[5] was introduced in a large container filled with 0.9 % NaCl and ρ was measured at 1 kHz, then, a PVC block (resistivity much larger than the saline solution, K = 1) attached to a micro-positioner was displaced along the perpendicular axis to the silicon probe and the ρ' values were obtained for various distances (x) and compared with those computed with the model (Figure 2.10). Observe that the experimental values fit quite nicely the predicted values by the model beyond 0.4 mm. Hence, it is possible to provide a value for the spatial resolution. For instance, if 1% resistivity measurement error is selected as a threshold, the spatial resolution would be 4 mm. That is, any medium disruption beyond 4 mm from the center of the silicon probe will cause measurement errors below 1%.

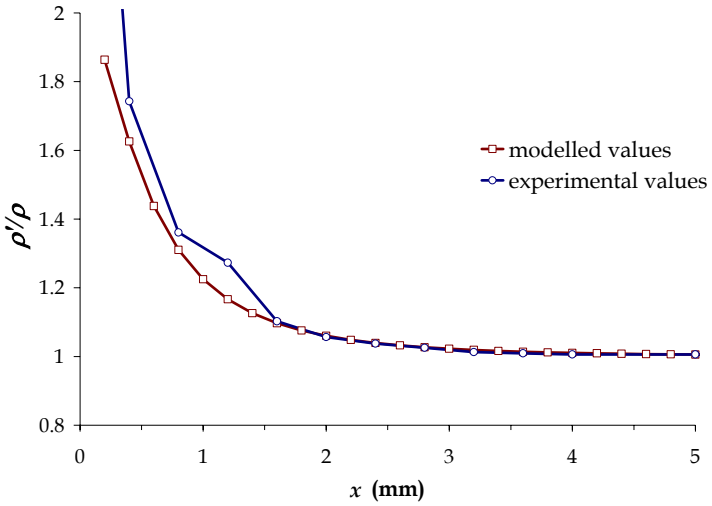

Figure 2.10. Expected and experimental ρ'/ρ values for the silicon probe.

The previous model assumed that the point-sized electrodes were completely surrounded by the medium 1. However, this is not true in the case of the needle probe since the electrodes are located on the needle surface and, therefore, a second 'reflective surface' should be considered. This fact probably explains the discrepancy that is observed (Figure 2.10) between the model and the experimental values for short medium-transition distances.

For very short distances it is possible to assume that this second medium transition is infinite extent and use a three-medium model. The third medium, above the electrodes, would correspond to the needle material and it can be assumed that its resistivity is infinite (Figure 2. 11). This model is especially suitable to estimate the effect of low resistivity disturbing layer, such as blood, on the electrodes. In this case, the medium of interest, 2, is separated from the electrodes by the disturbing layer, 1.

[5] The silicon probe used in this test was an intermediate design and its dimensions (a=0.8 mm and b=2.8 mm) were slightly different from the current probe (a=0.6 mm and b= 2.8 mm). See [23] for further details.

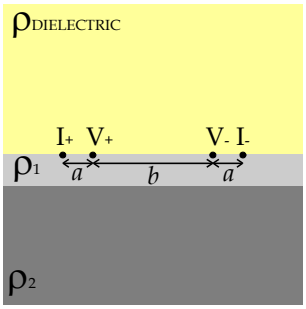

Figure 2. 11. Three media model.

By using the image method again, it is possible to obtain the expressions that relate the measured resistance (R) with the thickness (x) of the disturbing layer (ρ_1):

$$R = \frac{V}{I} = \frac{\rho_1}{2\pi}\left(2\left(\frac{1}{a} - \frac{1}{a+b}\right) + 4\left(\sum_{n=1}^{\infty} K^n \left[\frac{1}{\sqrt{a^2 + 4n^2x^2}} - \frac{1}{\sqrt{(a+b)^2 + 4n^2x^2}}\right]\right)\right) \tag{2.7}$$

$$K = \frac{\rho_2 - \rho_1}{\rho_2 + \rho_1} \tag{2.8}$$

Therefore, the apparent resistivity (ρ') largely depends on the thickens of the disturbing layer as it can be observed in Figure 2.12. Observe that the constant IESD configuration is less influenced by the disturbing layer than the non-constant IESD configuration chosen for the probe design.

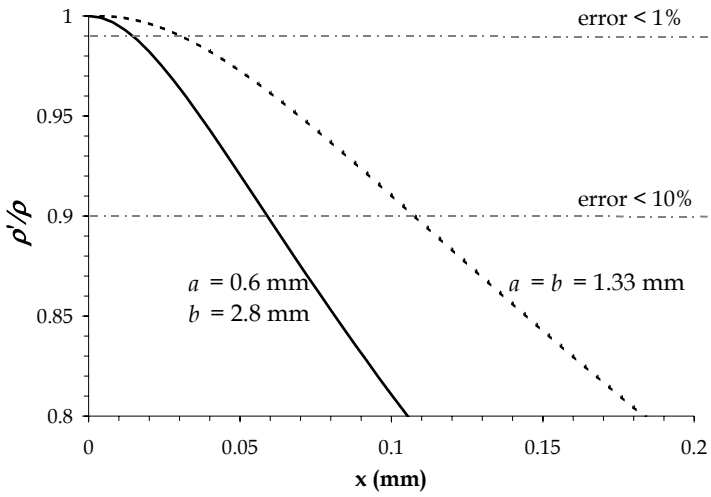

Figure 2.12. Dependence of ρ'/ρ on the thickness (x) of a low resistivity medium (ρ_1 = 100 Ω.cm) located between the electrode array and the medium under study (ρ_2 = 400Ω.cm).

Although the effect of a disturbing layer is of great relevance, it has been found experimentally that it rarely appears unless a blood vessel is damaged[6]. Therefore, it has been decided to keep the IESD as it was designed at the beginning of the MicroCard project.

As it has been mentioned, the above discussion assumed that the electrodes were point-sized and that is not at all the case of the MicroCard needle since the electrode dimensions are comparable to the separation distances. One conclusion that could be drawn from this fact is that a significant part of the current flows through the metal layer of the inner electrodes instead of flowing through the sample. As a consequence, the constant that relates the injected current, the measured voltage and the medium resistivity would be seriously modified and the above equations concerning the spatial resolution would be not valid. However, if the electrodes are thin and are sufficiently separated (separation distance equal or larger than the electrode size) the conduction through the electrodes does not significantly modify the situation as it shown by the following simulations: Figure 2.13 depicts the results from a bidimensional model equivalent to the MicroCard probe. Observe that the presence of the inner electrodes does not modify the current densities at the regions not close to the electrodes. Moreover, the voltage drop difference at the location of the inner electrodes only differs 1%.

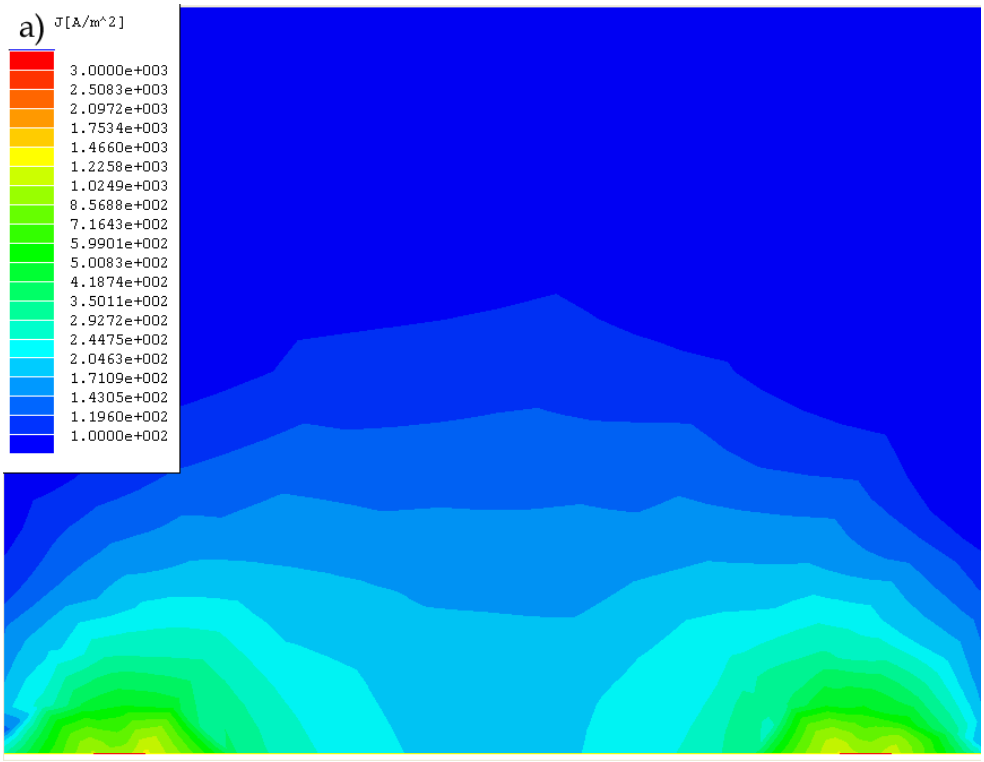

[6] In the case that a blood vessel is damaged, the measurements are so much distorted that it is clearly detected the effect of the disturbing layer and the user can decide to puncture in another location.

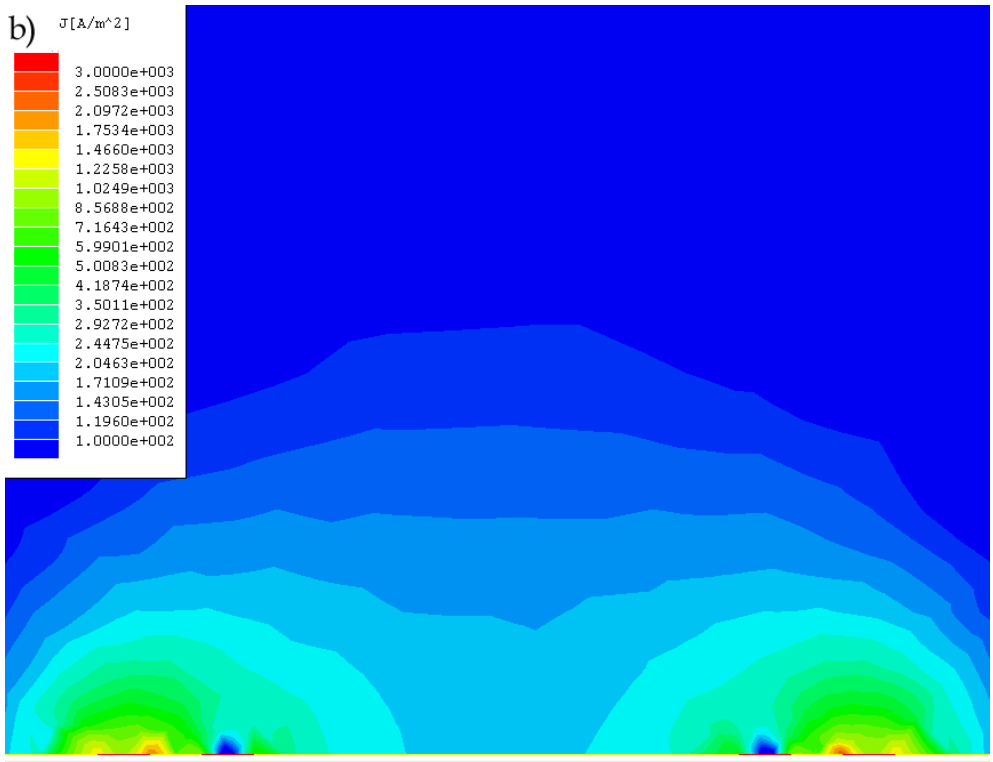

Figure 2.13. Bidimensional finite-element simulation (Maxwell 2D Student Version) of the current density distribution in the case of a) null size inner electrodes and b) inner electrodes equivalent to those of the MicroCard probe.

2.2.2. Electrode-tissue interface impedance

Living tissues, and more specifically the extracellular medium, can be considered predominantly as liquid electrolytes [28]. This implies that the charge carriers are ions and that electrons are bounded to their respective atoms and are not free to flow. Thus, in contrast to the *electronic* current in metals, tissue continuous currents are *ionic*. The transformation form electronic to ionic conduction occurs at the electrode-electrolyte interface[7]. Through chemical reactions (electrolysis) the electrode exchanges electrons with electrolyte species (ionization of neutral substances or neutralization of ions) and it is even possible that the electrode provides charged ions to the solution (oxidation reaction).

In most bioengineering applications, these electron exchange reactions are an undesired phenomenon since they can damage the tissue due to excessive accumulation of ions such as Cl^- or even degrade the electrode. Therefore, when possible, DC currents are avoided and *ideal polarized electrodes*[8] are employed. In those cases, AC currents are injected or measured through the *electrical double layer* that is formed at the electrode-electrolyte interface.

At the metallic phase of a electrode-electrolyte interface, any excess of charge resides at the surface and is compensated by a counter-charge in the electrolyte that also tends to reside at the surface. This creates the so called *electrical double layer* [29] that to some extent can be modeled by a capacitance. This ideal capacitive behavior has been observed in small-signal regime with liquid mercury electrode systems which have perfectly smooth surfaces. However, in many situations, especially with solid metal electrodes, the interface impedance is better modeled by the following equation for frequencies above 1 Hz [30]:

$$Z = K(j\omega)^{-\beta} \tag{2.9}$$

where K is a measure of the magnitude of Z and has units of $\Omega s^{-\beta}$, j is the complex number $(-1)^{1/2}$, ω is the frequency expressed in rad/s and β is an adimensional constant which has a value between 0 and 1, typically around 0.8 for many electrode systems. The fact that the phase angle ($\phi = \beta\pi/2$) is constant has led to the impedance being called a *constant phase angle*, CPA, or a *constant phase element*, CPE. In the case that $\beta=1$, the above impedance equation is equivalent to that of a capacitance. For lower β values the impedance can be seen as a frequency dependent capacitance. Therefore, the CPE is also known as a pseudo-capacitance.

[7] Some electrodes, such as standard ECG electrodes (Ag|AgCl electrodes), are composed by a metallic element and a salt or even an electrolytic gel. In those cases, the transformation from electronic to ionic conduction occurs inside the electrode, at the metal-electrolyte interface.

[8] At the metal-electrolyte interface of an ideal polarized electrode, also called ideally polarizable electrode, (IPE) no charge transfer occurs regardless of the potential imposed by an outside voltage source. No real electrode can behave as an IPE over the whole potential range available in a solution, however, some electrode-electrolyte systems, over a certain limited ranges (typically < 1V), can approach ideal polarizability.

For instance, Figure 2.14 shows the results from an impedance measurement at an oscillation voltage of 10 mV between two platinum electrodes of the MicroCard probe immersed in a NaCl 0.9% solution[9]. Its behavior has been modeled with a CPE (K=80×10^6 Ωs$^{-\beta}$, β = 0.83) in series with a resistance that accounts for the resistance of the connectors and wires and the resistive behavior of the solution. The observable disparity at high frequencies (>100 kHz) is caused by the parasitic capacitances and can be modeled by an small capacitance in parallel with the CPE+resistance model. In the case that the interface impedance is modeled by a capacitance (capacitive model), the results can be roughly approached by a capacitance of 4 nF, which gives a capacitance of 9 μF/cm^2 for each 0.0009 cm^2 platinum electrode of the probe[10].

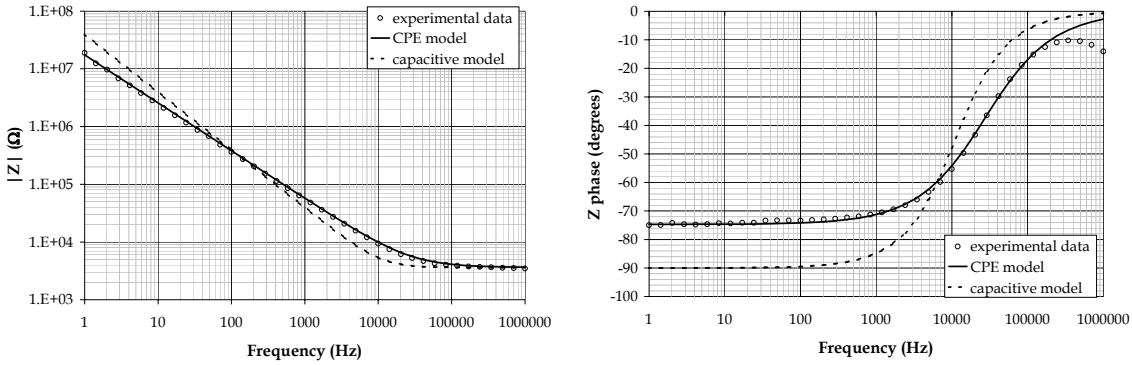

Figure 2.14. Experimental inter-electrode impedance module and phase in a NaCl 0.9% solution compared to its modeling by a constant phase element and a capacitance.

From Figure 2.14 it can be deduced that the transfer resistance, that is, the resistance that would model the charge transfer reactions, must be quite above 100 MΩ [11]. Thus, the assumption that MicroCard platinum electrodes are ideal polarized electrodes is reasonable. The equivalent circuit in the small signal AC regime for this case is depicted in Figure 2.15 where C_P models the parasitic capacitances, R_{S1} represents the resistance of the connectors and wires of electrode 1, Z_{CPE1} represents the electrode 1-electrolyte interface impedance, R_{SOL} is for the resistive behavior of the saline solution and R_{S2} and Z_{CPE2} account for the second electrode.

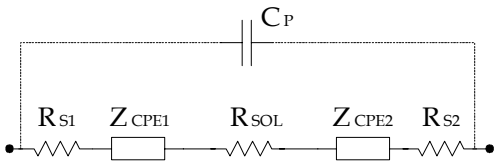

Figure 2.15. Small signal equivalent circuit for an inter-electrode measurement in a saline solution.

[9] Up to some tens of MHz the impedance behavior of such a solution is purely resistive.

[10] It must be taken into account that in this case two electro-electrolyte interfaces are is series.

[11] That does not mean that it is around 100 MΩ, it could be much larger. In fact, it has not been possible to measure the transfer resistance because of practical issues when measuring such large values.

In the case that the metal electrodes are connected to low impedance sources or sinks, the half-cell potentials[12] are of no relevance since the transfer resistances are very high. However, when the electrodes are connected to high-input impedance terminals, these potentials must be taken into account to avoid circuitry malfunction such as saturation due to unexpected DC voltages at the inputs. Although, in principle, the cell potential of two electrodes made of the same metal in an electrolyte should be equal to 0 V, impurities on the electrodes surfaces can produce different half-cell potentials that result in a voltage difference between the electrodes. By using a high input impedance voltmeter (MicropH 2002, CRISON INSTRUMENTS S.A.), voltage differences up to 0.5 V between two electrodes of the MicroCard probe have been measured. Moreover, these potentials are unstable and time evolutions such as that shown in Figure 2.16 are possible.

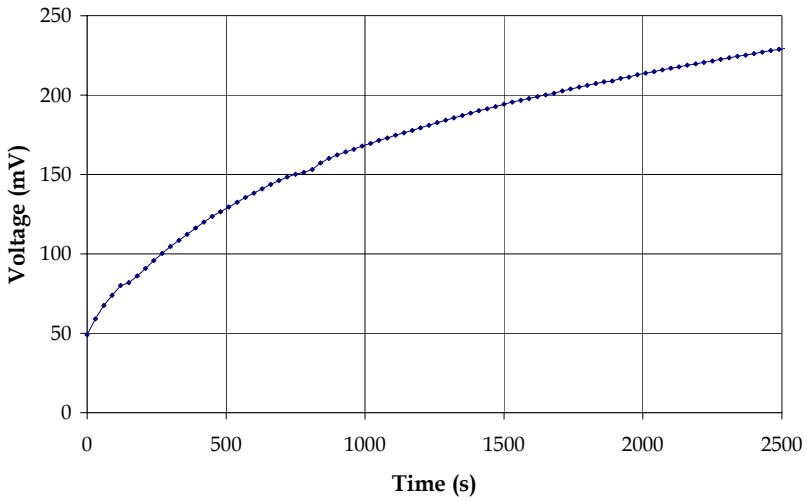

Figure 2.16. Open-circuit voltage measurement of a MicroCard electrode immersed in NaCl 0.9%.

2.2.3. Electrode platinization

As it is shown in next chapter, it is always desirable to keep the electrode-tissue interface impedance magnitude as low as possible, independently of the measurement method (two-electrode method or four-electrode method). As a consequence, a significant amount of time and effort has been invested to reduce such interface impedance during the MicroCard and MicroTrans projects.

In the case that enlargement of geometric size of the electrodes is not possible, reduced electrode-tissue interface impedance can be obtained by increasing the surface area

[12] Although some electrodes can almost be considered as IPEs, some degree of metal ions exchange between the metal and the electrolyte exists and that generates an electrical potential [31].

through control of electrode roughness. Mechanical methods, such as sandblasting, can be used to increase the roughness but impedance reduction is generally accomplished by electrochemical deposition of platinum onto the surface of the electrode in such a way that a black sponge-like or dendritic deposit results [32;33][13]. This greatly increases the surface area of the electrode and can reduce the interface impedance ten or more times, at low frequencies. Unfortunately, one of the problems encountered with platinum black coatings prepared from typical literature preparations is the relative frailty of the platinum deposition, which becomes easily detached when the electrode is inserted into the tissue. In the framework of this thesis work, the electrochemical deposition techniques were experimented and adjusted for the MicroCard probe electrodes.

Different adjustments and modifications were tried during the project but two general observations must be emphasized:

a) Previous studies [32] reported optimum current levels about 10 mA/cm^2 and optimum deposit charges from 30 to 60 A·sec/cm^2 for electrodes with areas larger than 1 mm^2. This is not the case of MicroCard electrodes (area = 0.09 mm^2) and the use of such 'optimum' levels resulted in poor impedance reduction or mechanical instability of the deposit (see Figure 2.17). It was found that higher current densities (500 mA / cm^2) and higher charges (related to the deposited mass) produced better results. This result agrees with the work performed by other researchers when working with sub-millimeter electrodes [34;35]

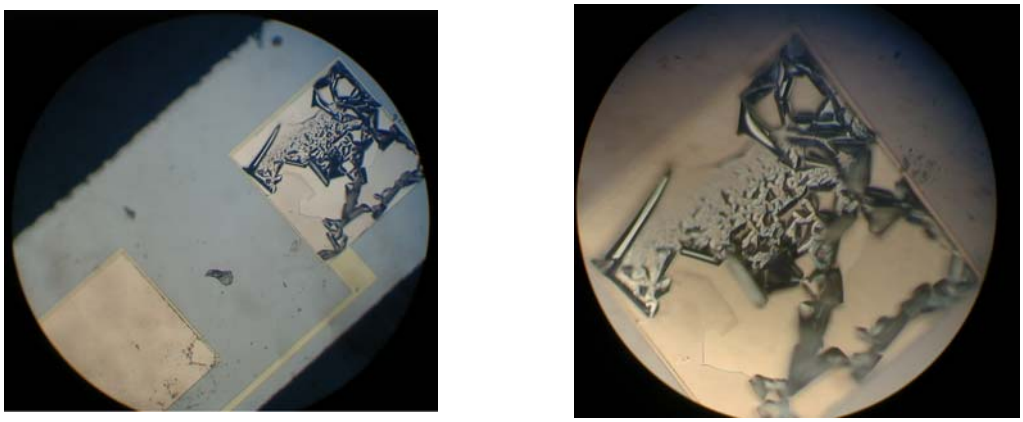

Figure 2.17. Micrographs of the electrode surfaces after platinization with insufficient current levels.

b) Mechanical stability is increased by performing some sort of 'natural selection' mechanism that rejects the platinum particles that do not attach strongly to the electrode surface. The first step was to use a pure mechanical cleaning method [36] and afterwards a method based on ultrasound agitation was employed [37]

[13] Nanotechnology could be also of great relevance in this field, it could provide techniques to increase the surface area.

Current platinization method

Materials:

- 'Kohlrausch solution': The electroplating solution consists of 10 ml distilled water, 0.3 g Cl_4Pt, 3 mg $Pb(CH_3COO)_2 \cdot 3H_2O$ (lead acetate 3-hydrate), and 0.25 ml HCl 0.1M [14].
- Anode: commercial platinum electrode (Radiometer Analytical). Its active volume is 5 mm × 4 mm × 0.3 mm
- Current source: custom made DC current source able to provide fixed currents (100 μA, 200 μA, 500 μA , 1000 μA). The maximum output voltage is +10 V.
- Ultrasound bath: stainless steel ultrasonic bath (1.75 l) operating at 25 kHz (Ref. LC20/H from ELMA, S.A.)

Process:

1) After a preliminary cleaning performed by brushing the probes with soft paper soaked in ethanol, the probe is immersed in ethanol and ultrasonic agitation is applied for three minutes.

2) The platinum electrodes are 'activated' to remove surface impurities: the probes are immersed in distilled water and a current of 500 μA is applied between each electrode pair for 1 minute (30 seconds for each polarity).

3) Electrochemical deposition of platinum black: a) 5 ml of the Kohlrausch solution are placed in a glass beaker (15 ml) that is adhered to the bottom of the ultrasonic agitation bath; b) the anode tip is introduced into the solution and it is connected to the positive pole of the current source: c) the probe is immersed in the solution; d) the ultrasonic bath is turned on; and e) each electrode is platinized during three minutes at 500 μA by connecting its corresponding wire to the negative pole of the current source[15].

4) Mechanical test: the probes are inserted repeatedly (50 insertions) in a polystyrene foam to test that the platinum deposit does not becomes easily detached. After an optical inspection, the electrical characterization is performed in a saline solution.

[14] All these products are acquired from Pamreac Química, S.A.

[15] Quite recently it has been tried to use a quadruple current source and to perform simultaneous platinization of the four electrodes. The results seem to be similar to those obtained with the sequenced electrode platinization method and the yield has been significantly improved. However, these are preliminary results and further analysis is required.

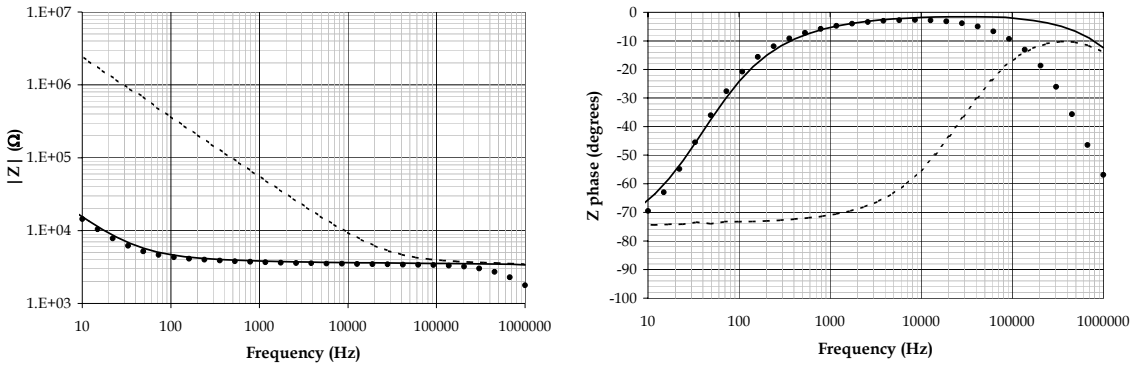

Figure 2.18. Inter-electrode impedance magnitude and phase angle in a NaCl 0.9% solution before platinization (dashed line), after platinization (continuous line) and after a series of *in vivo* tests (circumferences). The differences at high frequencies are due to a modification of the wiring system.

The characterization of the electrode interface impedance is performed by measuring the impedance between two distal electrodes of the probe immersed in saline solution (0.9% NaCl). The impedance magnitude and phase angle at an oscillation voltage of 10 mV from 10 Hz to 1 MHz is obtained by using a commercial impedance measuring system (SI 1260, Solartron Analytical from The Roxboro Group plc, Cambridge, UK).

As it can be observed in Figure 2.18, the platinization process reduces the interface impedance magnitude 100 or more times at low frequencies. Moreover, after a series of *in vivo*[16] tests, the electrode interface impedance still remains low denoting that the platinum deposit is sufficiently stable.

Probe storage in different environments[17] was tried but no significant differences were observed concerning the electrode interface impedance. The cleaning process before its usage seems more critical. It has been noticed that to rinse the probes in ethanol can be quite beneficial, particularly when the probes have been kept in air for some weeks.

2.2.4. Electrode-tissue interface impedance variability

Its is generally accepted that the electrode-electrolyte interface impedance in the case that the electrolyte is a biological tissue is quite similar to the 0.9% NaCl case. In fact, this solution has become a benchmark since its ionic content is equivalent to that of blood plasma.

However, the ionic concentrations of tissue and blood can be quite different during certain conditions, for example, during ischemia. Moreover, living tissues are heterogeneous at the scale of the MicroCard probe electrodes. Therefore, a great degree of variability should be expected in electrode-tissue interface impedances. Such a

[16] These *in vivo* tests correspond to the experimental study described in chapter 5.1
[17] Free air, distilled water and saline solution.

variability could compromise the quality of the measurements[18]. Thus, in order to study such a variability, we provided our tissue impedance measurement systems with a mechanism to measure the tissue-electrode impedance (see section C.2.2 in the annex C) and performed some *in vivo* and *ex vivo* experiments.

Figure 2.19 compares the tissue impedance magnitude (1 kHz, 5μA) with the electrode-tissue interface impedance magnitude in myocardium subjected to local ischemia. Two facts are noticeable: 1) the large scatter of interface impedance magnitude values (from 500 Ω to 3 kΩ) and 2) the interface impedance evolution is not correlated with the physiological event (ischemia)[19].

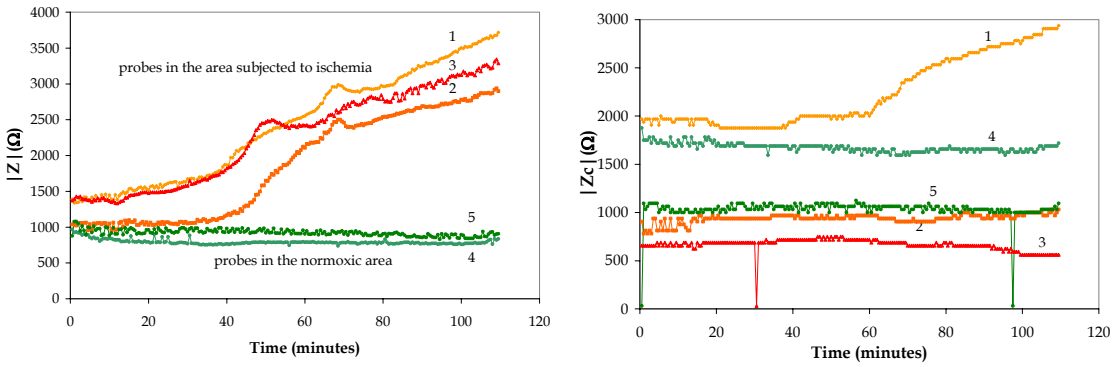

Figure 2.19. The figure on the left shows the tissue impedance magnitude (1 kHz, 5 μA_{RMS}) measured by using five MicroCard impedance probes in an isolated pig heart perfused by a Langendorff system [38]. Three of the probes (1,2 and 3) were inserted in an area subjected to local ischemia by clamping the left anterior descending artery while the others were inserted in a normally perfused area. The figure on the right shows the electrode impedance of the same probes. This experiment was carried out by the AMCA team.

In Figure 2.19, the wide range of values of the electrode-tissue interface impedance could be caused by the intrinsic tissue heterogeneity, by tissue heterogeneity caused by the local ischemia or by each electrode condition. However, considering the electrode size (300μm × 300μm) it is reasonable to think that the most important source of variability is the intrinsic heterogeneity of the tissue. In order to reinforce such hypothesis, another kind of experiment was performed: in an excised lamb kidney the same probe was repeatedly inserted (Figure 2.20). The long time period between the excision and the test (>24 hours, got from a butcher's shop) ensures that the physiological status is stable and homogeneous. The usage of the same probe ensures that the electrode condition is constant. Observe that the distribution of the interface impedance values is also quite wide and that both probes show similar results (mean value for Probe 1 is 12.9kΩ and mean value for Probe 2 is 12.2kΩ).

[18] As it is explained in the next chapter, the quality of the four-electrode impedance measurements not only depends on the interface impedance magnitude but also depends on the balancing of the inner electrodes interface impedances.

[19] That is an important justification of the four-electrode method against the two-electrode method: the electrode-tissue interface impedance is not correlated with the ischemia and, therefore, its influence on the measurement must be avoided.

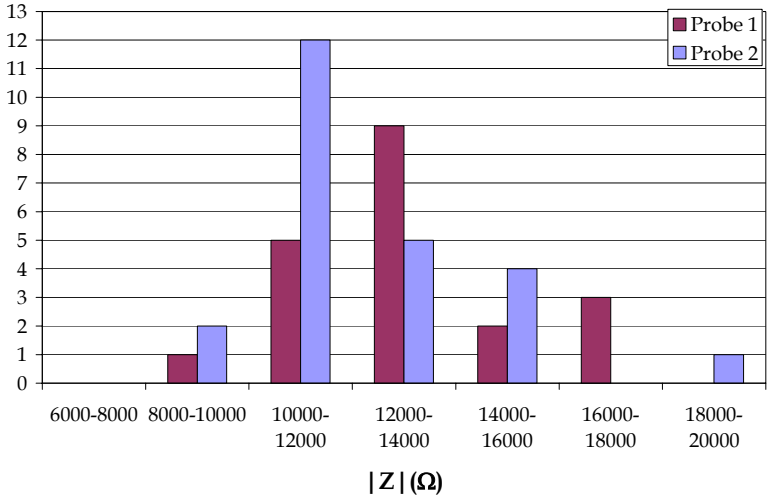

Figure 2.20. Histogram of tissue-electrode interface impedance magnitude values (1 kHz) obtained in an excised (>24 hours) lamb kidney at 15 ^{o}C. Both probes were inserted repeatedly in a homogenous area.

The above implies that each electrode in the same probe can show quite different electrode interface impedances when inserted into the living tissue. Therefore, it is confirmed that the convenient homogeneity of electrode impedances found in electrolyte solutions will not exist in the case of living tissues and that has important implications concerning the accuracy of the four-electrode impedance measurement method [39]. As it is shown in the next chapter, in the case that the electrode-tissue interface impedance variability is taken into account in the simulation of the four-electrode method, the acceptable lowest measurement frequency can increase from 10 Hz to 100 Hz.

2.2.5. Leakages through the silicon substrate

An unforeseen phenomenon when originally planning the MicorCard probes was the impedance measurement shunting caused by the silicon substrate. That is, part of the current injected from an electrode penetrates into the silicon substrate, through the non-passivated substrate surfaces (lateral surfaces), and travels through it to the vicinity of the colleting electrode where it leaves the silicon and enters the electrode. Figure 2.21 shows the experimental verification of this fact: two drops of saline solution (0.9% NaCl) on the electrodes of the probe are not in contact but allow the conduction through the substrate.

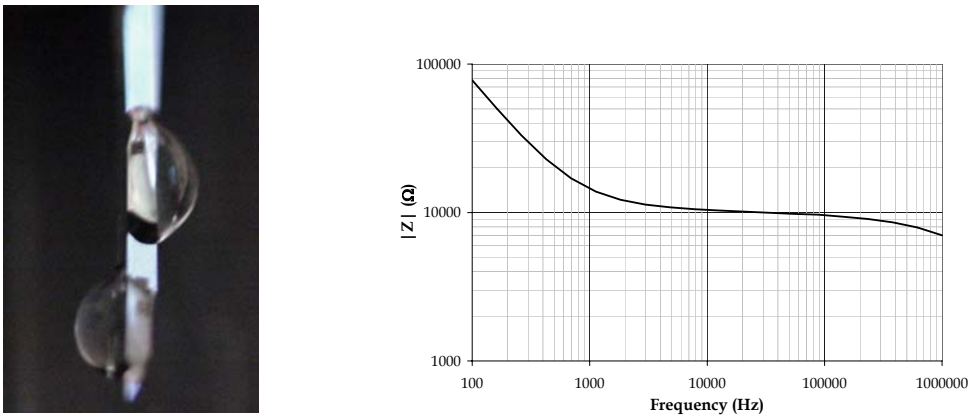

Figure 2.21. Impedance magnitude measured between external electrodes in the case that the current can only flow through the silicon substrate (the two saline drops on the left picture allow the electrode to silicon substrate conduction)

The effect of this parasitic phenomenon is not noticeable when measuring low resistivity solutions, such as 0.9% NaCl, since the solution-silicon interface offers much more resistance than the solution itself. However, when measuring higher resistivity solutions (e.g. 0.09% NaCl) this phenomenon is clearly manifested when performing four electrode measurements as it is shown in Figure 2.22. At low frequencies the conduction through the silicon substrate is not relevant since the silicon-solution interface behaves as any metal-electrolyte interface and, therefore, shows a very high interface impedance in comparison to the solution resistivity. However, at intermediate frequencies the conduction through silicon is significant and an impedance magnitude decrease is observed and an unexpected phase angle distortion is manifested.

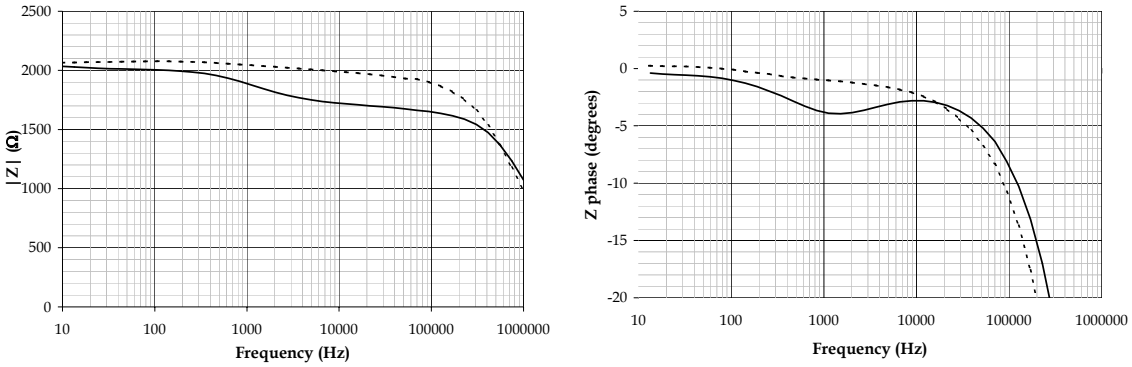

Figure 2.22. Four-electrode impedance magnitude and phase angle of a 0.09 NaCl solution in the cases of a standard probe (continuous line) and a probe with covered substrate surfaces (dashed line).

Because of the above, in the cases that high accuracy or multi-frequency measurements were required, the silicon substrate lateral surfaces were manually covered with a

biocompatible epoxy (OG603 from Epoxy Technology, Billerica,MA, USA) that minimizes the conduction through silicon (see Figure 2.22)[20].

2.3. Probes on flexible substrates

Although it has been demonstrated that the MicroCard silicon probes are suitable for *in vivo* measurements[21], it is evident that thinner probes based on flexible materials would be more appropriate to minimize tissue damage. The idea would be to develop the geometry of the probe on a thin flexible substrate that could be inserted into the tissue by using some sort of guide, such as an ordinary hypodermic needle, or that could be mounted on current instruments such as catheters.

The fact that the geometry of a flexible probe is not rigidly defined means that some degree of uncertainty in the constant cell will exist. In other words, since the probe can be flexed, the separation distances can be altered and, therefore, the voltage-current relationships can be modified. That implies severe constrictions to the measurement of resistivities. Fortunately, other parameters from the electrical bioimpedance characterization, such as the impedance phase angle, the characteristic frequency or α the parameter in the Cole model[22], are in principle constant cell independent and will not be affected by geometrical modifications in the case that the medium can be considered homogeneous and isotropic.

In the framework of MicroTrans project two flexible electrode designs were tested.

2.3.1. NIBEC probes

The Northern Ireland BioEngineering Centre (NIBEC) was one of the partners involved in MicroTrans and MicroCard projects and, among other issues, it was responsible for the development of probes on flexible substrates.

Departing from the CNM impedance probe designs, the NIBEC team developed probes on 25 μm thick polyimide substrates. The electrodes, the tracks and the bonding pads were made of gold (thickness= 0.2 μm) and an Iridium Oxide (IrO) deposition was applied on the electrodes for interface impedance reduction.

Unfortunately, it was not possible to achieve a sufficient interface impedance reduction (Figure 2. 23) and, what is worst, the IrO deposition was not stable and the interface impedance increased significantly during saline immersion which caused significant

[20] It is expected to solve this issue by using parylene coating [40], which is a process suitable for batch processing and commonly used for implants such as pacemakers. By now, the impedance probes produced for single-frequency measurements (1 kHz) do not include any kind of covering to avoid the conduction through silicon.

[21] See next chapters.

[22] Those parameters will be explained in the following chapters.

distortion of the four-electrode measurement, particularly at low frequencies (Figure 2.24).

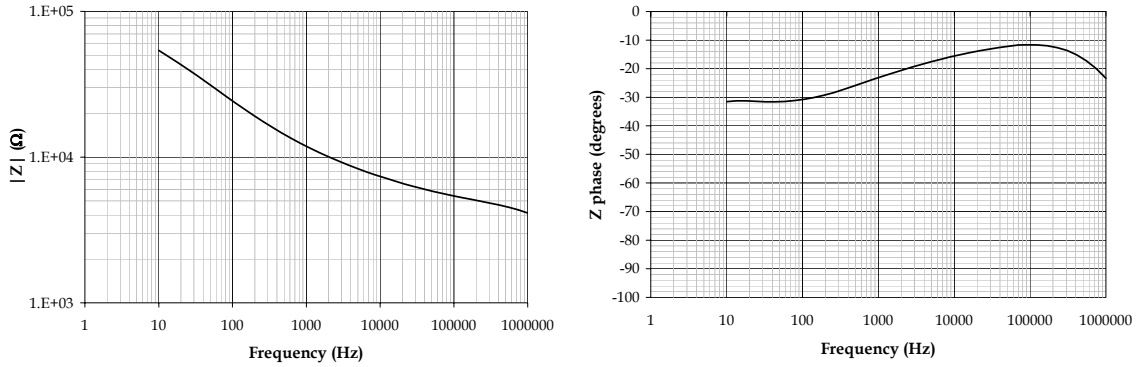

Figure 2. 23. NIBEC probe inter-electrode impedance magnitude and phase in a NaCl 0.9% solution.

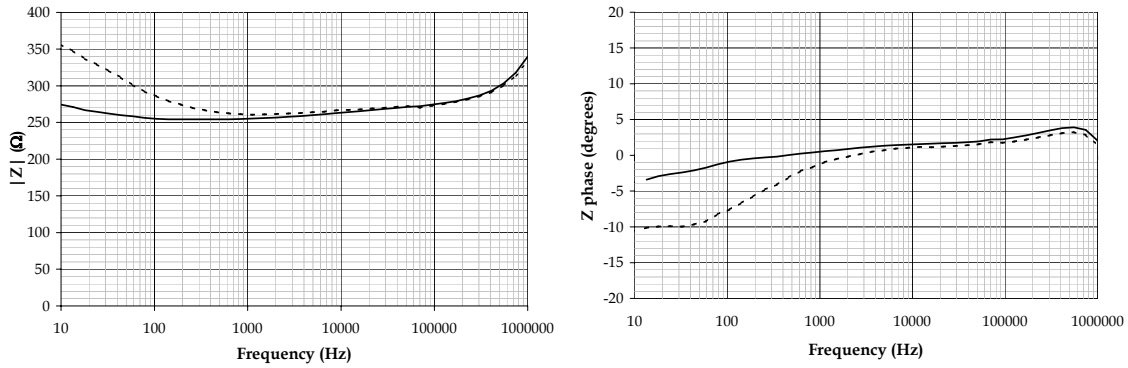

Figure 2.24. Four-electrode impedance magnitude and phase measurement of a saline solution (0.9% NaCl) performed with a NIBEC probe. The measurement after immediate immersion (continuous line) is reasonably fair but after 15 minutes (dashed line) it is severely distorted at low frequencies.

2.3.2. IBMT probes

The Fraunhofer Institute for Biomedical Engineering (IBMT) also develops electrode arrays on polyimide. Most of their designs are intended for neural recording or stimulation and none of them is specially thought for electrical bioimpedance measurements. However, it was decided to characterize some of them in order to assess whether or not they were useful for tissular bioimpedance measurements[23].

[23] These probes were provided by Medics Coordination Office (http://www.medics-network.com/). The reference of the probes is "Contact Array – Four Electrodes". They basically consists of a linear array of four electrodes (100 μm × 100 μm) at a constant separation distance (330 μm). It must be noted that quite recently [41] these probes have also been used by the IBMT researchers for impedance measurements.

First tests were performed with electrode arrays covered with Iridium - Iridium Oxide (Ir-IrO) for impedance reduction and potential stability [34]. The results indicated that the IrO layer did not provide the necessary low electrode interface impedance, probably because of its frailty. Fortunately, further tests with Pt-Pt black electrodes resulted in sufficiently low interface impedances (Figure 2.25) and four-electrode measurements were performed *in vitro* (Figure 2.26) and *in vivo* [24].

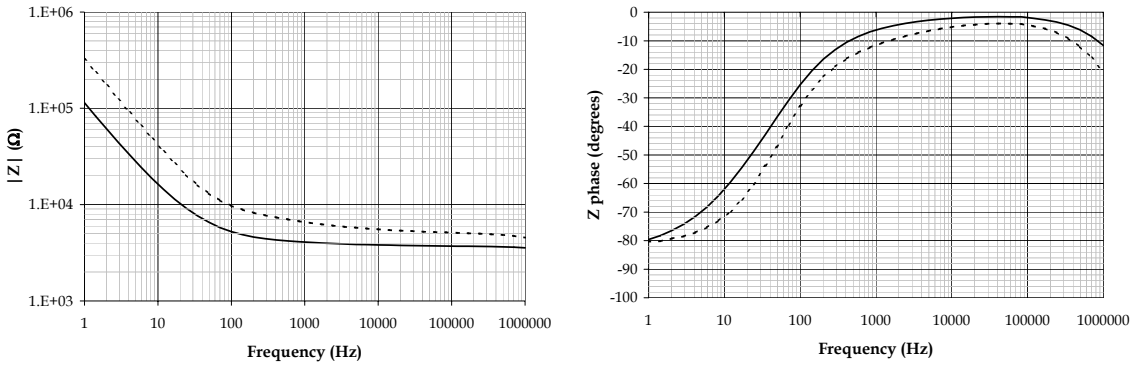

Figure 2.25. IBMT probe inter-electrode impedance magnitude and phase in a NaCl 0.9% solution before (continuous line) and after a prolonged in vivo test (dashed line).

Observe that the interface impedance measurements are comparable to those obtained with the MicroCard probe if it is taken into account than the IBMT electrode area (100 μm × 100 μm) is significantly lower than the MicroCard electrodes (300 μm × 300 μm). Although the interface impedance was significantly worsen after the *in vivo* test, it can be concluded that the electrodes of these probes are appropriate for single use applications.

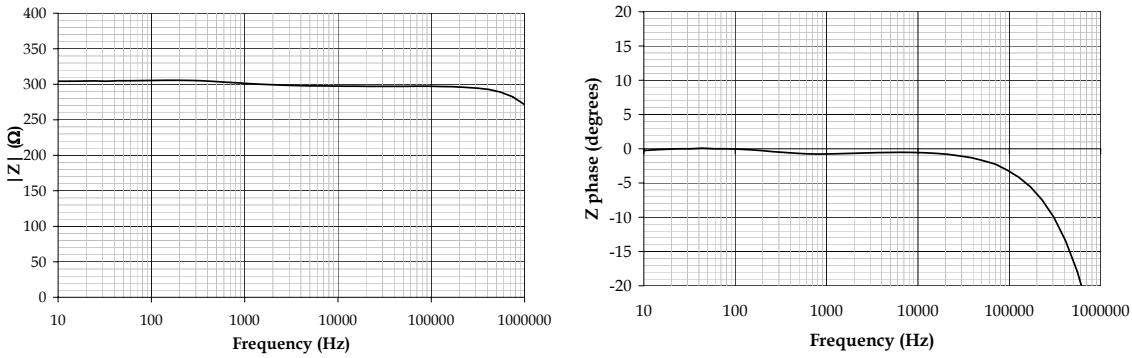

Figure 2.26. Four-electrode impedance magnitude and phase measurement of a saline solution (0.9% NaCl) performed with an IBMT probe.

[24] The *in vivo* test, more precisely *ex vivo* test, consisted in the continuous monitoring of an explanted rat kidney that was preserved in a cold preservation solution for more than 24 hours. Further details are provided in next chapters.

References

1. Tarjan, P. P. and McFee, R., "Electrodeless measurements of the effective resistivity of the human torso and head by magnetic induction," *IEEE Transactions on Biomedical Engineering*, vol. 15 pp. 266-278, 1968.

2. Casañas, R., Scharfetter, H., Altes, A., and Rosell, J. Magnetic induction system for non-invasive measurement of susceptibility and conductivity of biological tissues. 623-626. 2001. Oslo, norway. Proceedings of the XI International Conference on Electrical Bio-Impedance. 17-6-2001.
Ref Type: Conference Proceeding

3. Raicu, V., Saibara, T., and Irimajiri, A., "Dielectric properties of rat iver in vivo: a noninvasive approach using an open-ended coaxial probe at audio/radio frequencies," *Bioelectrochemistry and Bioenergetics*, vol. 47 pp. 325-332, 1998.

4. Morucci, J.-P., Valentinuzzi, M. E., Rigaud, B., Felice, C. J., Chauveau, N., and Marsili, P.-M., "Biolectrical Impedance Techniques in Medicine," *Critical Reviews in Biomedical Engineering*, vol. 24, no. 4-6, pp. 223-681, 1996.

5. Bao, J. Z., Davis, C. C., and Schmukler, R. E., "Impedance spectroscopy of human erythrocytes: system calibration, and nonlinear modeling," *IEEE Transactions on Biomedical Engineering*, vol. 40, no. 4, pp. 364-378, Apr.1993.

6. Geddes, L. A. and Baker, L. E., "Detection of Physiological Events by Impedance," in Geddes, L. A. and Baker, L. E. (eds.) *Principles of applied biomedical instrumentation* Thrid Edition ed. New York: Wiley-Interscience, 1989, pp. 537-651.

7. Steendijk, P., Mur, G., Van Der Velde, E. T., and Baan, J., "The Four-Electrode Resistivity Technique in Anisotropic Media: Theoretical Analysis and Application on Miocardial Tissue *in Vivo*," *IEEE Transactions on Biomedical Engineering*, vol. 40, no. 11, pp. 1138-1148, 1993.

8. Wtorek, J., Józefiak, L., Polinski, A., and Siebert , J., "An Averaging Two-Electrode Probe for Monitoring Changes in Myocardial Conductivity Evoked by Ischemia," *IEEE Transactions on Biomedical Engineering*, vol. 49, no. 3, pp. 240-244, 2002.

9. Rush, S., Abildskov, J. A., and McFee, R., "Resistivity of Body Tissues at Low Frequencies," *Circulation Research*, vol. XII pp. 40-50, 1963.

10. Schwartzman, D., Chang, I., Michele, J. J., Mirotznik, M. S., and Foster, K. R., "Electrical impedance properties of normal and chronically infarcted left ventricular myocardium," *Journal of Interventional Cardiac Electrophysiology*, vol. 3 pp. 213-224, 1999.

11. Fallert, M. A., Mirotznik, M. S., Downing, S. W., Savage, E. B., Foster, K. R., Josephson, M. E., and Bogen, D. K., "Myocardial electrical impedance mapping of ischemic sheep hearts and healing aneurysms," *Circulation*, vol. 87, no. 1, pp. 199-207, 1993.

12. Harms, J., Schneider, A., Baumgartner, M., Henke, J., and Busch, R., "Diagnosing acute liver graft rejection: experimental application of an implantable telemetric impedance device in native and transplanted porcine livers," *Biosensors & Biolectronics*, vol. 16 pp. 169-177, 2001.

13. Suesserman, M. F. and Spelman, F. A., "Quantitative *In Vivo* Measurements of Inner Ear Tissue Resistivities: I. In Vitro Characterization," *IEEE Transactions on Biomedical Engineering*, vol. 40, no. 10, pp. 1032-1047, 1993.

14. Cinca, J., Warren, M., Carreño, A., Tresànchez, M., Armadans, L., Gómez, P., and Soler-Soler, J., "Changes in Myocardial Electrical Impedance Induced by Coronary Artery Occlusion in Pigs With and Without Ventricular Arrhythmias," *Circulation*, vol. 96, no. 9, pp. 3079-3086, 1997.

15. Ellenby, M. I., Small, K. W., Wells, R. M., Hoyt, D. J., and Lowe, J. E., "On-line Detection of Reversible Myocardial Ischemic Injury by Measurement of Myocardial Electrical Impedance," *The Annals of Thoracic Surgery*, vol. 44 pp. 587-597, 1987.

16. Haemmerich, D., Ozkan, O. R., Tsai, J. Z., Staelin, S. T., Tungjitkusolmun, S., Mahvi, D. M., and Webster, J. G., "Changes in electricel resistivity of swine liver after occlusion and postmortem," *Med.Biol.Eng.Comput.*, vol. 40 pp. 29-33, 2002.

17. Tsai, J.-Z., Will, J. A., Hubbard-Van Stelle, S., Cao, H., Tungjitkusolmun, S., Cho, Y. B., Haemmerich, D., Vorperian, V. R., and Webster, J. G., "In-Vivo Measurement of Swine Myocardial Resistivity," *IEEE Transactions on Biomedical Engineering*, vol. 49, no. 5, pp. 472-483, 2002.

18. Tsai, J.-Z., Cao, H., Tungjitkusolmun, S., Woo, E. J., Vorperian, V. R., and Webster, J. G., "Dependence of Apparent Resistance of Four-Electrode Probes on Insertion Depth," *IEEE Transactions on Biomedical Engineering*, vol. 47, no. 1, pp. 41-47, 2000.

19. Blum, N. A. and Charles Jr, H. K. Multi-microelectrode probe for neurophysiological experiments. 15-18. 1988. Durham, NH, USA. Proceedings of the 14th Annual Northeast Bioengineering Conference. 10-3-1988.
Ref Type: Conference Proceeding

20. Drake, K. L., Wise, K. D., Farraye, J., Anderson, D. J., and Bement, S. L., "Performance of Planar Multisite Microprobes in Recording Extracellular Single-Unit Intracortical Activity," *IEEE Transactions on Biomedical Engineering*, vol. 35, no. 9, pp. 719-732, 1988.

21. Najafi, K., Ji, J., and Wise, K. D., "Scaling Limitations of Silicon Multichannel Recording Probes," *IEEE Transactions on Biomedical Engineering*, vol. 37, no. 1, pp. 1-11, 1990.

22. Yoon, T. H., Hwang, E. J., Shin, D. Y., Park, S. I., Oh, S. J., Jung, S. C., Shin, H. C., and Kim, S. J., "A Micromachined Silicon Depth Probe for Multichannel Neural Recording," *IEEE Transactions on Biomedical Engineering*, vol. 47, no. 8, pp. 1082-1087, 2000.

23. Ivorra, A., Aguiló, J., and Millán, J. Design considerations for optimum impedance probes with planar electrodes for bioimpedance measurements. 1, 269-272. 9-10-2001. Sinaia, Romania. International Semiconductor Conference, CAS 2001. 9-10-2001.
Ref Type: Conference Proceeding

24. Warren, M, "Electrical Impedance of Normal and Ischemic Myocardium. Role on the Genesis of ST Segment changes and Ventricular Arrhythmias." Ph.D. Thesis Universitat Autònoma de Barcelona, 1999.

25. "Introduction to Micro/Nanofabrication," in Bhushan, B. (ed.) *Springer handbook of nanotechnology* Berlin: Springer, 2004, pp. 147-184.

26. Robillard, P. N. and Poussart, D., "Spatial Resolution of Four Electrode Array," *IEEE Transactions on Biomedical Engineering*, vol. 26, no. 8, pp. 465-470, 1979.

27. Roth, B. J., "Interpretation of skeletal muscle four-electrode impedance measurements using spatial and temporal frequency-dependent conductivities.," *Med.Biol.Eng.Comput.*, vol. 27, no. 5, pp. 491-495, 1989.

28. Grimnes, S. and Martinsen, Ø. G., *Bioimpedance anb bioelectricity basics* London: Academic Press, 2000.

29. Bard, A. J. and Faulkner, L. R., *Electrochemical methods* New York: John Wiley & Sons, 1980.

30. McAdams, E. T., "Effect of surface topography on the electrode-electrolyte interface impedance, 1. The High Frequency (f>1 Hz), Small Signal, Interface Impedance - A Review," *Surface Topography*, vol. 2 pp. 107-122, 1989.

31. Grimnes, S. and Martinsen, Ø. G., *Bioimpedance and bioelectricity basics* London: Academic Press, 2000.

32. Geddes, L. A., *Electrodes and the measurement of bioelectric events* New York: Wiley-Interscience, 1979.

33. Feltham, A. M. and Spiro, M., "Platinized Platinum Electrodes," *Chemical Reviews*, vol. 71, no. 2, pp. 177-193, 1971.

34. Staiger, A., Schuettler, M., and Stieglitz, T. Impedanzsenkung flexiber Mikroelektroden durch galvanische Abscheidung von Platinum Black und Iridiumoxid (EIROF). 46, 500-501. 2001. Biomedizinische Technik. 35. Jahrestagung der Deutschen Gesellschaft für Biomedizinische Technik.
Ref Type: Conference Proceeding

35. Borkholder, D A, "Cell Based Biosensors Using Microlectrodes." PhD Thesis PhD Thesis, Stanford University, 1998.

36. Ivorra, A., Gómez, R., Noguera, N., Villa, R., Sola, A., Palacios, L., Hotter, G., and Aguiló, J., "Minimally invasive silicon probe for electrical impedance measurements in small animals," *Biosensors & Biolectronics*, vol. 19, no. 4, pp. 391-399, 2003.

37. Marrese, C. A., "Preparation of strongly adherent platinum black coatings," *Anal.Chem.*, vol. 59, no. 1, pp. 217-218, 1987.

38. Groot, J R de, "Genesis of life-threatening ventricular arrhythmias during the delayed phase of acute myocardial ischemia. Role of cellular electrical coupling and myocardial heterogeneities." PhD Thesis University of Amsterdam, 2001.

39. Pallás-Areny, R. and Webster, J. G., "AC instrumentation amplifier for bioimpedance measurements," *IEEE Transactions on Biomedical Engineering*, vol. 40, no. 8, pp. 830-833, Aug.1993.

40. Ratner, B. D. and Hoffman, A. S., "Thin films, grafts, and coatings," in Ratner, B. D., Hoffman, A. S., Schoen, F. J., and Lemons, J. E. (eds.) *Biomaterials Science* San Diego: Academic Press, 1996, pp. 105-130.

41. Cho, S. and Thielecke, H. Design of electrodes for impedance measurement of lesions in arteries. 351-354. 2004. Gdansk, Poland. Procedings from the XII International Conference on Electrical BioImpedance (ICEBI). 20-6-0004.
Ref Type: Conference Proceeding